EPR of Cu^{2+}-doped potassium oxalate monohydrate single crystal: Jahn-Teller effect and positions of Cu^{2+} ions

1991 J. Phys.: Condens. Matter 3 8479

(http://iopscience.iop.org/0953-8984/3/43/014)

J. Phys.: Condens. Matter 3 (1991) 8479–8489. Printed in the UK

EPR of Cu^{2+}-doped potassium oxalate monohydrate single crystal: Jahn–Teller effect and positions of Cu^{2+} ions

Sushil K Misra, Xiaochuan Li and Changlu Wang

Physics Department, Concordia University, 1455 de Maisonneuve Boulevard West, Montreal, Quebec, Canada H3G 1M8

Received 4 April 1991, in final form 24 June 1991

Abstract. X-band (~9.5 GHz) EPR measurements on a single crystal of Cu^{2+}-doped $K_2C_2O_4 \cdot H_2O$ (POM) have been carried out over the temperature interval 4.2–393 K. The data indicate the presence of four magnetically inequivalent Cu^{2+} sites, consisting of two pairs of physically equivalent sites. A study of the angular variation of the EPR line positions, and the variation of the EPR spectra with temperature reveal that Cu^{2+} ions belonging to one physically equivalent pair of sites exhibit pseudo-static and dynamic Jahn–Teller effects below and above 172 K, respectively, indicating that their local environment is nearly octahedral. The Cu^{2+} ions belonging to the other pair of physically equivalent sites do not exhibit a Jahn–Teller effect. An attempt has been made to determine the positions of the Cu^{2+} ions in the unit cell of POM. The principal values of the **g** and **A** matrices, as well as the orientations of their principal axes, for the two sets of physically equivalent Cu^{2+} ions, are evaluated from the positions of the allowed EPR hyperfine lines at 295, 77 and 4.2 K. In addition, the spin–lattice relaxation times of the Cu^{2+} ion in POM have been estimated from the EPR linewidths at various temperatures.

1. Introduction

A divalent copper ion (Cu^{2+}), when placed in an octahedral or nearly octahedral environment, provides the best known example of an ion undergoing Jahn–Teller distortion (Jahn and Teller 1937), which occurs when an ion is located at a site of sufficiently high symmetry such that a degenerate state would result for a rigid environment. In that case, the actual (elastic) environment spontaneously distorts itself to lift the degeneracy, arriving at a lower overall energy for the ion plus environment. When the kinetic energy of the ligand nuclei can be neglected, a static Jahn–Teller effect (JTE) is observed, otherwise a dynamic JTE manifests itself. Many occurrences of JTE have been reported for the Cu^{2+} ion in an octahedral symmetry, or in an octahedral symmetry with a small trigonal distortion, for which the Cu^{2+} ion possesses the twofold-degenerate ground state E_g (Misra and Wang 1989a, Silver and Getz 1974, Borcherts *et al* 1970, Petrashen 1980).

Potassium oxalate monohydrate, $K_2C_2O_4 \cdot H_2O$ (hereafter POM), belongs to a group of infrequently occurring crystal hydrates containing the minimum number of water molecules. EPR studies on Cu^{2+}-doped POM have been previously reported by Vinokurov *et al* (1976) at 300 and 77 K; they reported the observation of two types of spectra. However, they did not interpret the data to be indicative of the

0953-8984/91/438479+11$03.50

occurrence of JTE. Furthermore, their estimates of the spin-Hamiltonian parameters were not accurate, having been evaluated from the values of the extreme resonant line positions observed for only one orientation of the external magnetic field.

The present article reports more detailed EPR studies on a Cu^{2+}-doped POM single crystal over an extended temperature range (4.2–393 K), leading to the interpretation of the data in terms of occurrences of the pseudo-static and dynamic JTE for two of the four Cu^{2+} ions in the unit cell of POM, as inferred from the features of the temperature-dependent EPR spectra. The manifestation of the JTE has been exploited to distinguish between the various Cu^{2+} sites in the unit cell possessing different local symmetries. The Cu^{2+} spin-Hamiltonian parameters for the two pairs of physically equivalent Cu^{2+} ions in the unit cell are evaluated using a least-squares fitting procedure (Misra 1986, 1988). The spin-relaxation times (τ) for Cu^{2+} in the POM host have also been estimated at various temperatures.

2. Sample preparation and crystal structure

A $K_2C_2O_4 \cdot H_2O$ crystal is characterized by a monoclinic symmetry, belonging to the space group $C2/c$, with the unit-cell dimensions: $a = 0.9210$ nm, $b = 0.6165$ nm and $c = 1.0660$ nm; $\beta = 110.9°$ (Sequeira *et al* 1970, Pedersen and Holcomb 1963). The site symmetries at the potassium and water molecules are C1 and C2, respectively. The unit cell contains four formula units. The potassium ion is surrounded by eight oxygen atoms, out of which seven belong to four oxalate groups and one to the water molecule. The K–O distances range anywhere from 0.2745 to 0.3015 nm. Figure 1 shows the projection of the POM structure onto the (010) plane.

Single crystals of POM, doped with Cu^{2+}, were grown at room temperature by slow evaporation of a saturated aqueous solution of potassium oxalate, containing 0.5% by weight of $CuSO_4 \cdot 5H_2O$. The most developed faces in these crystals were found to be the (001), (111) and ($\bar{1}11$) faces (Misra and Wang 1989b). A crystal of size 1.5 mm × 1.0 mm × 2.5 mm was chosen for the present measurements.

3. Experimental arrangement and details of spectra

A Varian V4502 X-band spectrometer was used for recording EPR spectra. The magnetic-field values were determined by the use of a Bruker (B-NM20) gaussmeter. Diphenyl-picryl-hydrazyl (DPPH), for which $g = 2.0036$, was used as a reference to check the accuracy of resonant frequency and magnetic-field values; the line positions as determined from the graph had an accuracy of 0.5 G. The temperature was varied by means of a heater resistor inside the liquid-helium cryostat. For angular-variation studies, the excitation microwave field and the crystalline sample were kept fixed while the external magnetic (Zeeman) field was rotated.

The angular variations of the resonant line positions were recorded for the Zeeman field ($\boldsymbol{B}$) orientation in three mutually perpendicular planes at room (RT), liquid-nitrogen (LNT) and liquid-helium (LHT) temperatures. In each plane, the magnetic-field orientation was varied at 5° intervals. The most-even face, (001), i.e. the ab plane of the single-crystal specimen, was chosen to define the ZX-plane. The orientation of the principal axis corresponding to the largest principal g-value (the direction of the Zeeman field for which the positions of the lines are at the minimum) in this plane

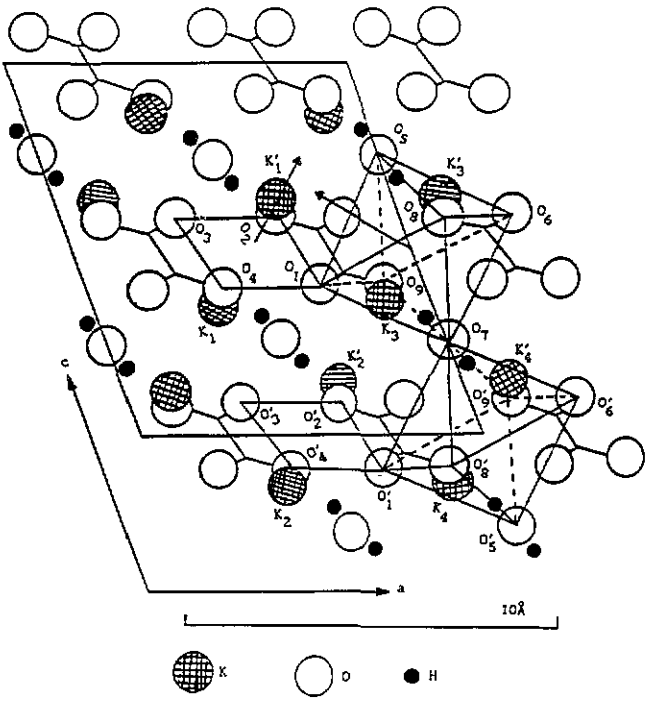

Figure 1. Projection of the POM crystal structure on to the {010} plane. The squares formed by $O_1O_2O_3O_4$ and $O_1'O_2'O_3'O_4'$ enclose Cu^{2+} ions 1 and 2, while the octahedra, as indicated, formed by $O_1O_5O_6O_7O_8O_9$ and $O_1'O_5'O_6'O_7'O_8'O_9'$ enclose Cu^{2+} ions 3 and 4, noting that O_7 and O_7' are the same.

was chosen to be the laboratory Z-axis, which was found to make an angle of ~33° with the a-axis. For EPR measurements in the laboratory ZY and XY planes the specimen was oriented in such a way that it could be rotated about the laboratory X- and Z-axes, keeping the Zeeman-field direction fixed.

3.1. EPR spectra at room and higher temperatures

At RT, since the Cu^{2+} ion has the electron spin $S = \frac{1}{2}$ and the nuclear spin $I = \frac{3}{2}$ for each of the ^{63}Cu (69.09% abundance) and ^{65}Cu (30.91% abundance) isotopes, two sets of four allowed Cu^{2+} hyperfine (HF) lines ($\Delta M = \pm 1, \Delta m = 0$; M and m are, respectively, the electronic and nuclear magnetic quantum numbers), overlapped by a weak, broad isotropic line, whose position was independent of the orientation of $\boldsymbol{B}$ (see section 3.2 for details), were observed for any Zeeman-field orientation in the laboratory ZX, ZY and XY planes. Except for the differences in the line intensities and the orientations of the respective principal axes, the two sets of spectra, consisting of four HF lines each, were found to be identical in all respects except for the orientations of their magnetic axes, i.e. they were magnetically inequivalent, but physically equivalent. These two sets correspond to the ions, presently referred to as Cu^{2+} ions 1 and 2. At RT, only the lowest- and highest-field HF lines corresponding to the two isotopes of copper were completely resolved, while the middle two lines were only partially resolved. The main features of the EPR spectra at temperatures higher than RT remained the same as those at RT. Spectra for the orientation of $\boldsymbol{B}$ in the XY

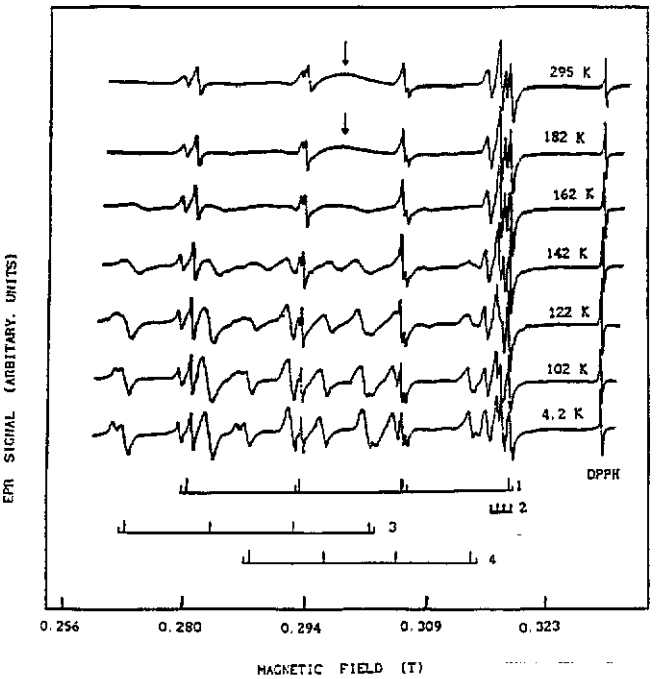

Figure 2. Temperature variation of Cu^{2+} EPR spectra in a POM single crystal for the Zeeman field, B, in the XY-plane, 20° away from the X-axis. The Cu^{2+} hyperfine lines due to the two isotopes (Cu^{63} and Cu^{65}) are clearly resolved at 102 K. For $T > T_{JT}$ ($T_{JT} = 172 \pm 2$ K), the two sets of the four HF lines, corresponding to two physically equivalent but magnetically inequivalent Cu^{2+} ions 3 and 4, merge to form a single broad and isotropic line, indicated by the arrow. For $T < T_{JT}$, the four sets of HF lines can be easily discerned. The HF lines belonging to the various Cu^{2+} ions for the spectra at 4.2 K have also been indicated.

plane, 20° away from the X-axis at various temperatures, are displayed in figure 2.

3.2. EPR spectra below room temperature

As the temperature was decreased from RT, the main features of the EPR spectra due to Cu^{2+} ions 1 and 2 in POM did not change significantly, implying that their spin-Hamiltonian parameters are temperature-independent (section 4). However, at and below $T_{JT} = 172 \pm 2$ K, two additional sets of four allowed Cu^{2+} HF lines appeared in place of the single broad and isotropic line above 172 K; their linewidths exhibited a significant change with temperature, as seen from figure 2, displaying the temperature variation of the Cu^{2+} EPR spectra. It was found that these two new sets of spectra were physically equivalent, but magnetically inequivalent, from each other. These correspond to the Cu^{2+} ions presently referred to as ions 3 and 4. The EPR spectra for Cu^{2+} ions 3 and 4 as observed above and below T_{JT} can be interpreted to be due to JTEs (for details see section 4). The angular variations of the resonant line positions corresponding to the four sets of spectra in the ZX plane at 4.2 K are plotted in figure 3.

3.2.1. Spin–lattice relaxation times. It is noted that the changes of the linewidths with temperature in the range 172–130 K for Cu^{2+} ions 3 and 4 are much more pronounced

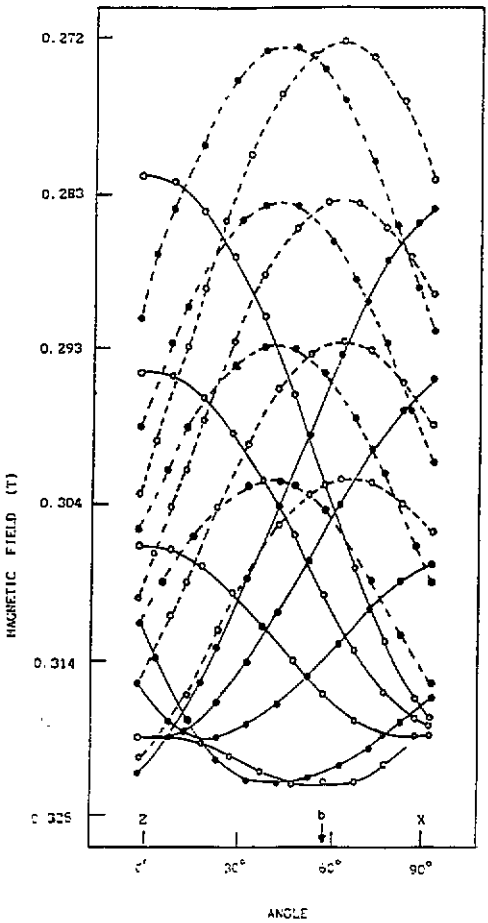

Figure 3. Angular variations of Cu^{2+} EPR line positions in POM at 4.2 K for the orientation of B in the laboratory ZX-, or the ab-plane. The full and broken curves connect data points corresponding to the same transition. Full curves with open and full circles correspond to Cu^{2+} ions 1 and 2 respectively, while broken curves with open and full circles represent Cu^{2+} ions 3 and 4, respectively.

than those for Cu^{2+} ions 1 and 2: the peak-to-peak first-derivative linewidth $\Delta B =$ 3.15 and 0.84 mT, for Cu^{2+} ions 3 or 4, at 162 and 4.2 K respectively, while $\Delta B = 1.01$ and 0.94 mT for Cu^{2+} ions 1 or 2, at RT and 4.2 K, respectively. The narrower linewidth is due to longer spin–lattice relaxation time of the impurity ion Cu^{2+} (τ_{Cu}) at lower temperature. τ_{Cu} can be estimated from the expression $\tau_{Cu} = \hbar/(g\mu_B\Delta B)$ (Abragam and Bleaney 1970, Breen *et al* 1969), neglecting the spin–spin interaction between Cu^{2+}–Cu^{2+} pairs. (Here μ_B and g are the Bohr magneton and the Cu^{2+} spectroscopic splitting factor respectively.) Accordingly, the values of τ_{Cu} for Cu^{2+} ions 3 and 4 in POM were estimated to be 1.66 and 6.22×10^{-9} s at 162 and 4.2 K, respectively, while for Cu^{2+} ions 1 and 2 $\tau_{Cu} = 5.23$ s and 5.62×10^{-9} s at RT and 4.2 K, respectively.

4. Spin-Hamiltonian parameters

The EPR line positions for a Cu^{2+} ion in POM were fitted to the following spin-Hamiltonian:

$$\mathcal{H} = \mu_B \boldsymbol{B} \cdot \mathbf{g} \cdot \boldsymbol{S} + \boldsymbol{S} \cdot \mathbf{A} \cdot \boldsymbol{I}. \tag{1}$$

The nuclear quadrupolar interaction has not been included in equation (1), since it has negligible effect on the allowed EPR line positions. In equation (1) $\boldsymbol{B}$ and $\mathbf{A}$ are the external Zeeman field and the HF-interaction matrix, respectively.

The principal values of the $\mathbf{g}^2(\equiv \mathbf{g}^T \cdot \mathbf{g})$ and $\mathbf{A}^2(\equiv \mathbf{A}^T \cdot \mathbf{A})$ tensors and their direction cosines were evaluated by a simultaneous fitting of all the EPR line positions, as observed for $\boldsymbol{B}$ in the three mutually perpendicular laboratory planes ZX, ZY and XY, for Cu^{2+} ion 1 at RT, LNT and LHT, and for Cu^{2+} ion 3 at LNT and LHT by the use of a least-squares fitting procedure (Misra 1986, 1988, Misra and Subramanian 1982). The principal values and direction cosines of the $\mathbf{g}$ and $\mathbf{A}$ matrices were so evaluated for Cu^{2+} ions 1 and 3, which are different from each other, at various temperatures; they are listed in tables 1 and 2, respectively. From the physical equivalence, it is concluded that the principal values of the $\mathbf{g}$ and $\mathbf{A}$ matrices for Cu^{2+} ions 2 and 4 are the same as those for Cu^{2+} ions 1 and 3, respectively.

It is seen from table 1 that the principal values of the $\mathbf{g}$ and $\mathbf{A}$ matrices for Cu^{2+} ion 1 remain the same, within experimental error, over the temperature range 4.2–295 K, while table 2 reveals that the principal values of the $\mathbf{g}$ and $\mathbf{A}$ matrices, for Cu^{2+} ion 3, change only insignificantly with temperature over the range 77–4.2 K.

5. Positions and local symmetry of Cu^{2+} ions in the lattice of POM

The observed EPR spectra were carefully studied, taking into account the structure of POM (Sequeira *et al* 1970), in order to deduce the most likely positions of the Cu^{2+} ions and the details of isomorphic substitution.

5.1. Positions and local symmetry of Cu^{2+} ions 1 and 2 in the lattice of POM

The orientation of the magnetic Z-axis for one of the Cu^{2+} ions 1 and 2 is nearly parallel to the K_1–K_1' line in figure 1, as determined by Vinokurov *et al* (1976), using the x-ray structural data. Therefore, from the physical equivalence of Cu^{2+} ions 1 and 2, the magnetic Z-axis for the other Cu^{2+} ion has been presently deduced to be most likely parallel to the K_2–K_2' line (figure 1). It should be noted here that the plane formed by the K_1–K_1' and K_2–K_2' vectors is the $(10\bar{1})$ plane. Further, the K_1–K_1' vector makes an angle of ~68° with the K_2–K_2' vector and the (010) plane bisects the (K_1–K_1', K_2–K_2') angle. For charge compensation, it is necessary to assume isomorphic substitution by a Cu^{2+} ion for two K^+ ions. This assumption is consistent with the fact that the superhyperfine (SHF) splitting due to the interaction of the Cu^{2+} ions with the ligand protons belonging to the water molecules has not yet been observed. If a positional substitution of a K^+ ion by a Cu^{2+} ion had indeed occurred, a resolved SHF structure should have been observed, at least for some orientations of $\boldsymbol{B}$. In order for the EPR data for Cu^{2+} ions 1 and 2 to be consistent with the crystal structure, the two Cu^{2+} ions 1 and 2 should have the same ligand environment and be located in between the four oxygens O_1–O_2–O_3–O_4, at the position (0.5, 0.5, 0.5), and in

Table 1. Principal values and direction cosines of the principal axes of the **g** and **A** matrices for Cu^{2+} ion 1 in POM single crystal at 295, 77 and 4.2 K; these principal values are the same as those for Cu^{2+} ion 2 in POM. Here, the listed values are the averages of those estimated for the isotopes ^{63}Cu and ^{65}Cu. The principal values of **g** are dimensionless, while those of **A** are expressed in GHz. The indicated errors are those estimated by the use of a statistical method (Misra and Subramanian 1982). The direction cosines of the principal axes of the **g** tensor (X', Y', Z') are given with respect to the X-, Y- and Z-axes defined in section 3, while those of the **A** tensor (X'', Y'', Z'') are expressed relative to (X', Y', Z').

Temperature (K)	Principal value	Direction cosine		
		Z/Z'	X/X'	Y/Y'
295	$g_{Z'} = 2.3330 \pm 0.0040$	0.6904	0.0537	−0.7214
	$g_{X'} = 2.0721 \pm 0.0040$	0.6661	0.3415	0.6630
	$g_{Y'} = 2.0663 \pm 0.0040$	0.2820	−0.9383	0.2000
	$A_{Z''} = 0.4832 \pm 0.0050$	0.9938	0.0444	−0.1016
	$A_{X''} = 0.0486 \pm 0.0050$	0.0317	0.9637	0.0644
	$A_{Y''} = 0.0504 \pm 0.0050$	0.1063	−0.0643	0.9576
77	$g_{Z'} = 2.3306 \pm 0.0040$	0.6727	0.0593	−0.7375
	$g_{X'} = 2.0831 \pm 0.0040$	0.5625	0.6885	0.4576
	$g_{Y'} = 2.0665 \pm 0.0040$	0.4806	−0.7227	0.4965
	$A_{Z''} = 0.4384 \pm 0.0050$	0.9988	0.0981	−0.2421
	$A_{X''} = 0.0448 \pm 0.0050$	0.0218	0.9156	0.1430
	$A_{Y''} = 0.0454 \pm 0.0050$	0.2318	−0.1289	0.9328
4.2	$g_{Z'} = 2.3405 \pm 0.0040$	0.6705	−0.0085	−0.7417
	$g_{X'} = 2.0931 \pm 0.0040$	0.4972	0.6001	0.4095
	$g_{Y'} = 2.0801 \pm 0.0040$	0.4340	−0.5742	0.3829
	$A_{Z''} = 0.4417 \pm 0.0050$	0.9861	0.1850	−0.1431
	$A_{X''} = 0.0432 \pm 0.0050$	0.0981	0.8871	−0.1011
	$A_{Y''} = 0.0467 \pm 0.0050$	0.4371	−0.1069	0.8932

between the four oxygens O_1'–O_2'–O_3'–O_4' at the position (0.5, 0.5, 0.0) (figure 1). This implies substitution by a Cu^{2+} ion in place of two nearest-neighbour K^+ ions (K_1–K_1' or K_2–K_2' as indicated in figure 1). It is noted that the x-ray data indicate that the oxygen atoms O_1, O_2, O_3 and O_4 belonging to the two oxalate groups very nearly form a square around the position (0.5, 0.5, 0.5) (Vinokurov *et al* 1976), and the O_1', O_2', O_3' and O_4' oxygen atoms from the other two oxalate groups form another square around the position (0.5, 0.5, 0.0), as indicated in figure 1.

5.2. Positions and local symmetry of Cu^{2+} ions 3 and 4 in the lattice of POM

In order for the EPR spectra due to Cu^{2+} ions 3 and 4, which exhibit JTE (section 6), to be physically equivalent to each other and conform to structural data, the sites of Cu^{2+} ions 3 and 4 should be located in the middle of the two distorted-coordination octahedra formed by the O_1–O_5–O_6–O_7–O_8–O_9 and O_1'–O_5'–O_6'–O_7'–O_8'–O_9' oxygen atoms, at the positions (1.0, 0.5, 0.5) and (1.0, 0.5, 0.0), respectively, as exhibited in figure 1. This requires substitution by a Cu^{2+} ion in place of two nearest-neighbour monovalent K^+ ions (K_3–K_3' or K_4–K_4' in figure 1), which lie close to the faces of the

Table 2. Principal values and direction cosines of the principal axes of the **g** and **A** matrices for Cu^{2+} ion 3 in POM single crystal at 77 and 4.2 K; these principal values are the same as those for the Cu^{2+} ion 4. Here, the principal values of the **A** matrix represent the averages of those for the ^{63}Cu and ^{65}Cu isotopes. For more details, see the caption of table 1.

Temperature (K)	Principal value	Direction cosine		
		Z/Z'	X/X'	Y/Y'
77	$g_{Z'} = 2.4155 \pm 0.0040$	0.3691	0.6894	0.6231
	$g_{X'} = 2.1291 \pm 0.0040$	−0.3676	0.7241	−0.5834
	$g_{Y'} = 2.0367 \pm 0.0040$	−0.8535	−0.0136	0.5208
	$A_{Z''} = 0.3675 \pm 0.0050$	0.8900	0.2541	0.0328
	$A_{X''} = 0.0001 \pm 0.0050$	−0.1970	0.8679	−0.4381
	$A_{Y''} = 0.0987 \pm 0.0050$	−0.2651	0.5021	0.8519
4.2	$g_{Z'} = 2.4367 \pm 0.0040$	0.3406	0.6566	0.6729
	$g_{X'} = 2.1339 \pm 0.0040$	−0.3250	0.7538	−0.5710
	$g_{Y'} = 2.0499 \pm 0.0040$	−0.8822	−0.2421	0.4702
	$A_{Z''} = 0.3607 \pm 0.0050$	0.8218	0.4271	0.0067
	$A_{X''} = 0.0002 \pm 0.0050$	−0.1042	0.7752	−0.3525
	$A_{Y''} = 0.0992 \pm 0.0050$	−0.3428	0.6549	0.8026

coordination octahedra. The magnetic Z-axes of the Cu^{2+} ions 3 and 4 coincide with the quasi twofold axes of the distorted octahedra.

A local octahedral symmetry is required at the sites of Cu^{2+} ions 3 and 4 for the occurrence of JTE (section 6). When a Cu^{2+} ion 3 or 4 substitutes for two K^+ ions, it introduces a local distortion of the original complex due to its position being different from those of the two host K^+ ions. This distortion is further augmented by the Jahn–Teller distortion caused by the Cu^{2+} ion. Due to these two distortions, the three principal values of the **g** matrices of Cu^{2+} ions 3 and 4 in POM all differ from each other at temperatures below T_{JT}, indicating a lower, orthorhombically distorted octahedral, symmetry at the site of Cu^{2+} ions 3 and 4. On the other hand, the two principal values of the **g** matrix for Cu^{2+} ions 1 or 2 in POM are equal to each other, within experimental error, because of the higher local symmetry seen by them than that exists for Cu^{2+} ions 3 and 4.

6. Jahn–Teller effect

When the paramagnetic Cu^{2+} ion is introduced into the lattice of POM, substituting for two K^+ diamagnetic ions, local distortions are introduced because the size, location and magnetic nature of the Cu^{2+} ion are different from those of the two replaced K^+ ions. This leads, as seen in section 6.1, to the occurrence of a pseudo-static JTE.

6.1. Pseudo-static JTE below 172 K

The two conditions necessary for the occurrence of the JTE are (Callaway 1976):

(i) the Cu^{2+} ion should be introduced at a site of local symmetry so that it results in a degenerate electronic ground state; and

(ii) it should occupy a minimum-energy non-degenerate state consequent to the small local distortion of the lattice that it causes.

Details of the pseudo-JTE exhibited by $[Cu(H_2O)_6]^{2+}$ complexes have been described by Petrashen *et al* (1980), and by Misra and Wang (1990). The following details apply to the present case. The complexes formed by Cu^{2+} ions 3 and 4 in POM possess orthorhombically distorted octahedral symmetry. Thus, they exhibit a pseudo JTE, which can be described as follows. According to crystal-field theory, the orbital doublet E_g of the Cu^{2+} ion becomes split in a field of orthorhombic symmetry, the lower state being either $|X^2 - Y^2\rangle$ or $|3Z^2 - r^2\rangle$. In the present case, the predominant ground state of the Cu^{2+} ion is $|X^2 - Y^2\rangle$, with an admixture of the excited state $|3Z^2 - r^2\rangle$, because the value of R ($\equiv (g_x - g_y)/(g_z - g_x)$) is less than 1 (Misra *et al* 1990). The splitting between the $|3Z^2 - r^2\rangle$ and $|X^2 - Y^2\rangle$ energy levels is sufficiently small, in the present case, to allow a significant mixing of the two substates of E_g by coupling with the lattice vibrations. The vibronic mixing of these close-lying (pseudo-degenerate) levels due to the interaction of the Cu^{2+} ion with its ligands manifests itself in the so-called pseudo-static JTE (Bersuker and Polinger 1984). Had these levels been degenerate, they would have resulted in the static JTE.

The interpretation of the EPR spectra of Cu^{2+} ions 3 and 4 in POM below 172 K, in terms of the pseudo-static JTE, wherein the lowest-lying levels of the E state lie extremely close to each other but are not degenerate, is equivalent to that of the 'static' JTE, wherein the lowest-lying levels are degenerate, the degeneracy being lifted by a Jahn–Teller distortion (Abragam and Bleaney 1970). This is similar to the case of an E-state ion by Bir (1976) for a tetragonally distorted octahedral Cu^{2+} complex, such as $[Cu(H_2O)_6]^{2+}$.

The molecular and electronic structures of the complex formed by the Cu^{2+} ion and its six ligands, is conventionally described in terms of Jahn–Teller coupling between the two close-lying substate of E_g and vibrational (ϵ_g) states of the orthorhombically distorted octahedral complex (Bersuker and Polinger 1984). The harmonic–vibrational potential, together with linear coupling terms, gives rise to the well known Mexican-hat potential surface (Abragam and Bleaney 1970). The geometry of the Cu^{2+} complex fluctuates between the conformations of symmetries D_{4h} and D_{2h}, which are generated by linear combinations of $Q_\theta (= \rho \cos\phi)$ and $Q_\epsilon (= \rho \sin\phi)$, which are the components of the ϵ_g vibrational mode. When higher-order coupling terms are included, the perimeter of the Mexican hat becomes warped, yielding three equivalent minima whose projections correspond to different ϕ values in the (Q_θ, Q_ϵ) space. Ham (1972) pointed out that a strain, similar to that which is prevalent in the present case as indicated by the three different principal values of the **g** matrices for Cu^{2+} ions 3 and 4 in POM, displaces the energies of the three configurations with respect to each other, thereby destroying their equivalencies. It is, therefore, expected that for Cu^{2+} ions 3 and 4 in POM, one of the three inequivalent valleys lies much lower than the other two, because one of the principal g values is significantly different from the other two (table 2). When only the lowest potential valley is occupied at low temperatures, i.e. when $\Delta E > k_B T$ (ΔE is the energy difference between the lowest and the next-lying potential valleys), the principal values of the **g** matrix of the Cu^{2+} ions 3, or 4, are not expected to be very temperature-dependent, in accordance with the present data. Further, in the present case, only one set of four HF lines, for each of the two magnetically inequivalent Cu^{2+} ions 3 and 4 was observed, implying that only the lowest potential valley is occupied. For, otherwise, as seen in the case of Cu^{2+}-doped

$Zn(C_4H_4N_2)SO_4 \cdot 3H_2O$ single crystal (Misra and Wang 1989a), three magnetically inequivalent sets of Cu^{2+} HF lines corresponding to the three potential valleys should have been observed for each magnetically inequivalent Cu^{2+} ion.

6.2. Dynamic JTE above 172 K

Above 172 K, the HF lines corresponding to Cu^{2+} ions 3 and 4 in POM became much broader because of decreased spin–lattice relaxation time (τ_{Cu}). At higher temperatures, k_BT is not smaller than ΔE, the separation between the two lowest-lying Jahn–Teller potential valleys. When $k_BT \gg \Delta E$, the Boltzmann populations of the three potential valleys are almost equal. This results in a single isotropic line, consistent with the present observation of a broad isotropic EPR line for $T > T_{JT}$ ($= 172 \pm 2$ K). This is characteristic of type-I dynamic JTE (Ham 1972), which occurs when the rate of tunnelling through the barrier from one distorted configuration of the Cu^{2+} complex to the other exceeds the frequency difference between the corresponding EPR resonance lines for the different distorted configurations, i.e. that between the anisotropic spectra (Ham 1972). From the time-averaging effect, when dynamic JTE occurs, $g_Z = g_X = g_Y = g_e - 4\lambda/\Delta$, where g_e (2.0023) is the g-value of the free electron, λ is the spin–orbit coupling constant for the free Cu^{2+} ion ($= -830$ cm^{-1}) and Δ is the octahedral crystal-field parameter for the Cu^{2+} ion. Thus, the value of $(g_e - \lambda/\Delta) = 2.20$, assuming the typical value of $\lambda/\Delta = -0.05$ for the Cu^{2+} ion (Abragam and Bleaney 1970). This value is very close to the observed g-value (2.194 ± 0.004) for the isotropic broad line at $T \geqslant T_{JT}$. Further, it is equal to the average of the three principal values of $\mathbf{g}$ ($= 2.193$) for Cu^{2+} ions 3 and 4 at $T < T_{JT}$, thus confirming the occurrence of type-I dynamic JTE (Ham 1972).

Since the EPR line positions and linewidths of Cu^{2+} ions 3 and 4 in POM are independent of the orientation of $\boldsymbol{B}$ at higher temperatures ($T > T_{JT}$), the strengths of the 'oriented' and 'random' strains can be considered to be very small compared with k_BT. This is in accordance with the fact that the centre of an EPR line depends on the orientation of $\boldsymbol{B}$ if the 'oriented' strains are large, while the width of an EPR line depends on the orientation of $\boldsymbol{B}$ if the 'random' strains are dominant (Ham 1972).

7. Concluding remarks

In addition to evaluating the principal values and orientations of the principal axes of the $\mathbf{g}^2$ and $\mathbf{A}^2$ tensors, as well as the spin–lattice relaxation times of the Cu^{2+} ion, the salient features of the present EPR study on a Cu^{2+}-doped POM single crystal can be described as follows.

(i) Four magnetically inequivalent Cu^{2+} sites, consisting of two pairs of physically equivalent ions, were observed. Upon entering the POM lattice, a Cu^{2+} ion enters in place of two K^+ ions. Thus, two types of Cu^{2+} sites are possible; one of these is characterized by a local orthorhombically distorted octahedral symmetry, as indicated by the three different principal values of the $\mathbf{g}$ matrix for the Cu^{2+} ion at this site at temperatures lower than 172 ± 2 K. The other type of possible site is characterized by a higher local symmetry, characterized by two principal values of the $\mathbf{g}$ matrix being almost equal to each other for this site in the temperature range 4.2–295 K.

(ii) The EPR spectra for Cu^{2+} ions 3 and 4 in POM are consistent with the occurrences of Jahn–Teller effects; below 172 ± 2 K a pseudo-static JTE was observed, while at temperatures above 172 ± 2 K a type-I dynamic JTE was observed.

Acknowledgments

The authors are grateful to the Natural Sciences and Engineering Research Council of Canada for partial financial support (grant no OGP0004485) and to the Concordia University Computer Center for providing their facilities to analyse the data.

References

Abragam A and Bleaney B 1970 *Electron Paramagnetic Resonance of Transition Ions* (Oxford: Clarendon)

Bersuker I B and Polinger V Z 1984 *The Dynamical Jahn-Teller Effect in Localized Systems* (Amsterdam: North-Holland)

Bir G L 1976 *Sov. Phys.–Solid State* **18** 946

Borcherts R H, Kanzaki H and Abe H 1970 *Phys. Rev.* B **2** 23

Breen D P, Krupka D C and Williams F I B 1969 *Phys. Rev.* **179** 241

Callaway J 1976 *Quantum Theory of the Solid State* (New York: Academic)

Ham F S 1972 *Electron Paramagnetic Resonance* ed S Geschwind (New York: Plenum)

Jahn H A and Teller E 1937 *Proc. R. Soc.* A **161** 220

Misra S K 1986 *Magn. Reson. Rev.* **10** 285

—— 1988 *Physica* B **151** 433

Misra S K and Subramanian S 1982 *J. Phys. C: Solid State Phys.* **15** 7199

Misra S K and Wang C 1989a *J. Phys.: Condens. Matter* **1** 771

—— 1989b *Phys. Rev.* B **39** 8832

—— 1990 *Mag. Reson. Rev.* **14** 157

Pedersen B and Holcomb D F 1963 *J. Chem. Phys.* **38** 61

Petrashen V E, Yablokov Y V and Davidovich R L 1980 *Phys. Status Solidi* b **101** 117

Sequeira A, Srikanta S and Chidambaran R 1970 *Acta Crystallogr.* B **26** 77

Silver B L and Getz D 1974 *J. Chem. Phys.* **61** 638

Vinokurov V M, Bulka G R, Gainullina N M and Nizamutdinov N M 1976 *Sov. Phys. Crystallogr.* **21** 434